The Effects of morpholine pre-treated and carboxymethylated cellulose nanofibrils on the properties of alginate-based hydrogels

Amaka J. Onyianta [a, *], Maila Castellano [b], Mark Dorris [a], Rhodri L. Williams, Silvia Vicini [b, *]

[a] *Material Chemistry and Processing, School of Engineering and Built Environment, Edinburgh Napier University, Edinburgh, EH10 5DT, United Kingdom*

[b] *Department of Chemistry and Industrial Chemistry, University of Genoa, Genoa, 16146, Italy*

* Corresponding authors

E-mail addresses a.onyianta@napier.ac.uk (A.J. Onyianta), silvia.vicini@unige.it (S. Vicini)

Abstract

The effects of varying percentage loadings of morpholine pre-treated cellulose nanofibrils (MCNF) and carboxymethylated cellulose nanofibrils (CMCNF) on the aqueous swelling, compressive modulus and viscoelastic properties of calcium-ion-crosslinked alginate hydrogels were investigated. In addition, the pore structure of hydrogels with the highest compressive modulus were studied. The incorporation of 5 wt. % MCNF resulted in a slightly reduced aqueous swelling, a 36 % increase in compressive modulus and a layered pore structure when compared with the neat alginate hydrogel. On the other hand, the addition of CMCNF at the same loading led to a slightly improved aqueous swelling, an increase in compressive modulus (17 %) and high porosity. Further increases in CNF loadings did not result in significant increase in material properties. The alginate/CNF composite materials have potentials to be used in applications where good swelling and mechanical robustness are required.

Highlights

- The effects of two types of CNF on alginate hydrogels were studied.
- Aqueous swelling of the hydrogels was affected by the CNFs' surface properties and amounts.
- Mechanical properties of the alginate hydrogels were improved by the addition of CNF.
- The porosity of the hydrogels was influenced by the type of CNF.

Keywords Hydrogels, alginates, cellulose nanofibrils (CNF), carboxymethylation, surface modification, compressive modulus.

1. Introduction

Polysaccharidic biopolymers such as alginates, cellulose, chitosan, chondroitin sulphate and hyaluronic acid are widely researched for applications in biomedical (Aravamudhan, Ramos, Nada, & Kumbar, 2014), pharmaceutical/drug delivery (Cardoso, Costa, & Mano, 2016), packaging (Hubbe, Ferrer, Tyagi, Yin, & Salas, 2017), and agricultural fields (Guilherme et al., 2015). These materials provide potentials for low cost and sustainable products because of their ubiquitous sources of extraction. Moreover, their inherent non-toxic, biocompatible and biodegradable properties have made them well recommended in biomedical applications for bone and tissue regeneration (Park, Lih, Park, Joung, & Han, 2017), wound care dressings (Leppiniemi et al., 2017) and for the delivery of various drugs and growth factors (Aravamudhan et al., 2014; Augst, Kong, & Mooney, 2006).

Naturally occurring in seaweed and brown algae, Sodium Alginate (SA) is a linear unbranched polymer consisting of β-D-mannuronic acid (M) and α-L-guluronic acid (G) arranged in a chain sequence of MM-GG-MG (Augst et al., 2006). The presence of carboxyl groups on the surface of SA promotes hydrophilicity and solubility in water. These carboxyl groups can also engage in ionic crosslinking with divalent ions such as Ca^{2+} and Ba^{2+} in the well-known “egg-box” model to form relatively stable network structures. The properties of the resulting network structure are influenced by the type of crosslinking ions, concentration of crosslinking ions, temperature, time and method of gelation (Kuo & Ma, 2001; Vicini, Mauri, Wichert, & Castellano, 2017).

Calcium ions are mostly used for the ionic crosslinking of SA. These ions have been introduced internally within the SA solution from a slurry of $CaCO_3$-D-glucono-δ-lactone system (Kuo & Ma, 2001), diffused from internally dispersed Ca^{2+} enriched microbeads (Vicini, Castellano, Mauri, & Marsano, 2015; Vicini et al., 2017), diffused from a bath of $CaCl_2$ solution (Ma et al., 2017) or sprayed onto the SA solution (Lin et al., 2014). The internal gelation method for SA crosslinking has been noted to provide more controlled gelation compared to the external gelation/diffusion method, which usually results in a spontaneous and heterogeneous material, characterised by a hard outer shell and a soft inner core (Kuo & Ma, 2001). To reduce the rate of diffusion and gelation, Bajpai et al. (2016) added SA solution to 8 kDa molecular weight cut off filtration membrane, before crosslinking in a bath of $CaCl_2$. The study shows that the gelation process started from the outer circumference of the SA

solution before gradually diffusing into the inner core. However, the homogeneity of the resulting hydrogel prepared using this method was not investigated.

Regardless of the gelation method used for the crosslinking of sodium alginate, the use of lower concentration of crosslinking ions leads to a material with high moisture absorbance and low mechanical properties. Increasing the concentration of the crosslinking ions however result to a material with low swelling and high mechanical properties (Augst et al., 2006). High mechanical and good swelling properties are desirable properties in the fields of biomedicine. In order to achieve the properties that would be fit for specific applications, many studies have focused on formulating blends of alginate with synthetic and naturals polymers (Kong & Mooney, 2003; Lee et al., 2004; Lin et al., 2014). These alginate-based composites can be formulated in the form of films, sponges and hydrogels (Augst et al., 2006). Being a three-dimensional network material, hydrogels are capable of absorbing large amount of solvent without dissolving and are therefore topical materials for various biomedical applications (Ahmed, 2015).

Nanocellulose is a nano-sized cellulose material extracted in the form of rod-like crystals (cellulose nanocrystals, CNC) and nanofibrils (cellulose nanofibrils, CNF) using various chemical (Onyianta, Dorris, & Williams, 2018), enzymatic (Beyene et al., 2017) and mechanical pre-treatments followed by mechanical processing (Abdul Khalil et al., 2014). It is a renewable, biocompatible and biodegradable biopolymer with improved mechanical strength, lightweight properties, optical properties, barrier properties and structuring capabilities (Jonoobi et al., 2015; Klemm et al., 2011). Hence, the increased industrial and research interests on nanocellulose for wide range of applications. Some of the chemical pre-treatment methods such as carboxymethylation (Wågberg et al., 2008), 2,2,6,6-tetramethylpiperidine-1-oxyl (TEMPO)-mediated oxidation (Isogai, Saito, & Fukuzumi, 2011), and quaternisation (Aulin, Johansson, Wågberg, & Lindström, 2010) modify the surface of the cellulose, thereby imparting new properties which are different from the original cellulose material. Onyianta et al. (2018) compared the properties of cellulose nanofibrils prepared using three types of chemical pre-treatment methods. The study shows that the presence or absence of surface charge on the CNF is responsible for the changes in crystallinity, viscoelasticity, thermal properties and aspect ratios of these CNF materials.

Interest in SA/nanocellulose blends in particular has increased, mainly because of the reinforcing capability of nanocellulose (Huq et al., 2017; Lin et al., 2014; Ma et al., 2017;

Smyth et al., 2018). These blends of SA and nanocellulose are mostly prepared by external gelation method, which is a fast gelling method with possible areas of localised gelation. In addition, the carboxyl groups on the TEMPO-oxidised nanocellulose has been reported to participate in the crosslinking process with Ca^{2+} ions (Lin, Bruzzese, & Dufresne, 2012). However, studies on how the presence or absence of surface charge of the CNF and varying amounts of CNF affect the elastically effective crosslinking chains of SA hydrogel are still lacking.

In this study, slower diffusion and homogeneous crosslinking of SA hydrogels were prepared using calcium chloride enriched agar wells, a method adapted from Stagnaro, Schizzi, Utzeri, Marsano, & Castellano (2018). The effect of temperature and duration of crosslinking on the homogeneity of the neat alginate hydrogels were initially studied. Subsequently, the effects of unmodified and surface modified cellulose nanofibrils on the surface interaction, equilibrium swelling, storage modulus, compressive modulus and morphology of alginate hydrogels were investigated. The modified Flory's equation (Flory, 1953) for the deformation of a swollen polymer network, based on the affine network model was then used to calculate the effect of the two types of CNF on the elastically effective chains of SA hydrogels at varying loadings. The affine network model assumes that macromolecular deformation of a network structure directly translates to the deformation of the elastically effective chains within the structure. This model has been used to characterise the elastically effective crosslinking degree of other hydrogel materials from natural and synthetic origins (Muniz & Geuskens, 2001; Sannino et al., 2005).

2. Experimental

2.1 Materials

Medium viscosity SA from brown algae, with molecular weight ranging from 80,000 to 120,000 g/mol and composed of approximately 61% mannuronic and 39% guluronic acids (M/G ratio of 1.56), calcium chloride ($CaCl_2$) and sodium chloride (NaCl) were used as received from Sigma-Aldrich. Agar powder by BD Difco™ was used for the gel moulds. Two types of aqueous CNF suspensions (1 wt. %) were used to prepare SA_CNF dispersions at different loadings relative to the amount of SA solid content. The first CNF was produced using aqueous morpholine pre-treatment before the mechanical processing (MCNF) and has negligible surface charge. The second CNF was prepared by carboxymethylation pre-treatment

before the mechanical processing (CMCNF) and has 550 µmol/g of anionic carboxymethyl groups on its surface. The details and material properties of the two types of CNF used in this study are well described previously by Onyianta et al. (2018). Deionised water was used throughout the experiment.

2.2 Preparation of SA solution and SA_CNF dispersions

2 wt. % SA solution was prepared as a control by dissolving the appropriate amount of SA powder in water under continuous stirring for not less than 2h using a magnetic stirrer. 100 g SA_CNF dispersions were prepared by weighing out appropriate amounts of CNF suspension into a beaker and diluted with the required amount of water and stirred. A constant mass of 2 g SA powder was then added to the diluted CNF suspension to make 2 wt. % SA having 5, 10 and 20 wt. % MCNF or CMCNF relative to the dry mass of SA, designated as SA_MCNF_5, SA_MCNF_10, SA_MCNF_20, SA_CMCNF_5, SA_CMCNF_10 and SA_CMCNF_20. The increment in CNF loading was by multiples of 2.

2.3 Preparation of agar gel moulds and SA_CNF hydrogels

Agar powder was added to 0.5 M $CaCl_2$ solution at 1 wt. % and brought to boil to dissolve the agar. 15 g of the solution was weighed into small 55 x 15 mm petri-dishes and allowed to gel at room temperature for not less than 2 h. After complete gelation of the agar solution, cylindrical glasscutter with 28 mm internal diameter was used to create wells within the agar gels. 4.5 g of SA solution or SA_CNF dispersions were then added into the wells created within the agar gels. A rectangular glass slab was gently placed on top of the SA solution to prevent bulging of the gels during crosslinking and to maintain the cylindrical shape of the hydrogels. At the end of the crosslinking process, which was visually assessed by a change from translucent light brownish colour to opaque light brownish colour, the gels were thoroughly washed in deionised water and swollen to an equilibrium state.

2.4 Equilibrium swelling of the never-dried hydrogels in water

The never-dried hydrogels were swollen in water to an equilibrium point, with the aim of characterising the network structure of the hydrogels. The mass of the equilibrium swollen hydrogel and the oven dried mass were recorded and used for the calculation of the swelling degree using the relationship given in Equation 1.

$$\text{Swelling degree} = \left(\frac{W_s - W_d}{W_d}\right) \qquad \text{Equation 1}$$

Here, W_d is the dry mass of the hydrogel and W_s is the swollen mass of the hydrogel.

2.5 Homogeneity Test

A facile homogeneity test (Kuo & Ma, 2001) was initially carried out on the equilibrium swollen neat SA hydrogels to study the effect of the crosslinking temperature and duration on the uniformity of the crosslinks formed within the hydrogels. the tests were carried out at 4 °C, 25 °C and 37 °C for 24h, 48h and 72h. Since the crosslinking process occurred by diffusion of the calcium ions from the agar gel into the SA solution, it is therefore expected that the outer circumference of the SA solution in the mould would be crosslinked before the inner circumference. The cylindrical hydrogels were cut perpendicularly into three approximately equal masses and labelled as 1, 2, and 3 as shown in the photographic insert in Fig. 1. The aliquot hydrogels labelled 1 and 3 were mainly composed of the outer geometry of the hydrogels, while the aliquot labelled 2 was composed of the mid portion of the hydrogel. Afterwards, the aliquots were dried and the polymer weight fraction, which is the ratio of dry cut to swollen cut was reported.

2.6 Fourier transform infrared spectroscopy (FTIR) analysis

The interaction between the alginate and the two types of CNF at different loadings were studied from dried samples using Spectrum 100 FTIR (Perkin Elmer, USA), in the attenuated total reflectance (ATR) mode. Spectral data were collected from 4000 to 500 cm^{-1} after 8 scans.

2.7 Rheological measurements of the hydrogels

The viscoelastic properties of the equilibrium swollen hydrogels were analysed using a 25 mm parallel plate geometry on MCR 301 rheometer (Anton Paar, Austria). A limited amplitude sweep was first conducted from 0.001 % to 0.2 % shear strain at 1 Hz frequency in order to determine the Linear Viscoelastic Region (LVR). This is the region where the microstructural response and associated viscoelastic properties of a material are independent of the degree of deformation imposed (Goodwin & Hughes, 2008). This was followed by three frequency sweeps: an initial sweep from 1 Hz to 10 Hz, followed by a second sweep from 0.1 Hz to 50 Hz and finally a third sweep from 1 Hz to 10 Hz, all carried out at 0.01% shear strain. The repeated frequency sweeps were carried out to verify whether the samples are within their linear viscoelastic region during the frequency sweeps. This should appear as an overlap of the three

frequency sweeps. Each sample was tested in duplicates. Since the three frequency sweep regimes were overlapping for all the samples, only the average of the second frequency sweep (0.1 Hz to 50 Hz) is hereby reported.

2.8 Mechanical measurements of the hydrogels by uniaxial compression tests

The equilibrium-swollen hydrogels were carefully cut with an 8 mm diameter metal cutter in a pool of deionised water just before the compression tests to prevent water loss by drying. The sample height varied between 5.3 to 6.2 mm with an average diameter of 8 mm. The samples were compressed to 4.3 – 5.2 mm (compression gap of 1 mm) at a velocity of 100 µm/s using an 8 mm parallel plate geometry (PP8) on MCR 301 rheometer (Anton Paar, Austria). The upper platen was gently lowered until the normal force was between 0 N and 0.1 N. The normal force-displacement data obtained from the rheometer was transformed to stress-deformation factor data using Equations 2 and 3. The deformation factor is related to strain but considers the dimensional (*x*, *y*, *z*) changes upon compression (Flory, 1953). The compressive modulus (*G*) was calculated as the slope of the linear region from the plot of stress vs deformation factor as shown in Equation 4. An average value of *G* from five compression tests is hereby reported for each sample.

$$\sigma = F/A \qquad \text{Equation 2}$$

$$\gamma = -(\lambda - \lambda^{-2}) \qquad \text{Equation 3}$$

$$G = \sigma/\gamma \qquad \text{Equation 4}$$

Here, σ is the compressive stress, *F* is the normal force, A = (πr^2) is the cross-sectional area of the sample geometry, in this case a cylinder, γ is the deformation factor, and λ is the ratio of the final height of sample to the initial height, known as the compression ratio.

Using the data from compression tests and equilibrium swelling in water, the elastically effective chains of the hydrogels, ν_e (mol/cm^3) were determined. This is the chain ends that are connected to the active crosslinks within the hydrogel network. This method of determining the elastically effective chains is based on the affine network model, which assumes that crosslinks are firmly connected to the elastic body, and elastically effective chains deform in the same manner with the macroscopic body (Akagi et al., 2011). ν_e was calculated for each sample using the modified version of Flory's equation for the deformation of swollen network (Flory, 1953) given in Equation 5 as obtained from Muniz & Geuskens (2001).

$$\nu_e = G \,/\, RT(\phi_r/\phi_s)^{2/3}\phi_s \qquad \text{Equation 5}$$

Here, G is the compressive modulus in Pa, R is the universal gas constant (8.314 x 10^6 cm^3 Pa mol^{-1} K^{-1}), T is the absolute temperature (293 K), ϕ_r is the volume fraction of the polymer in the relaxed state, i.e., the hydrogel formed in the agar mould after the excess $CaCl_2$ has been leached and ϕ_s is the volume fraction of polymer at equilibrium swollen state. The volume of SA, CNF and water were converted from their weights using the density of SA (1.6 g/cm^3), cellulose (1.5 g/cm^3) and water at 20 °C (0.9982 g/cm^3).

2.9 Morphological assessment

Morphological investigations of the cross-sections of freeze-dried SA, SA_MCNF_5 and SA_CMCNF_5 were carried out using a field emission scanning electron microscope (FE-SEM), ZEISS SUPRA 40 VP. The freeze-dried equilibrium swollen hydrogels allow the probing of the network structure created within the hydrogel during the crosslinking process. Prior to image analysis, all samples were obtained by fragile fractures in liquid nitrogen and were thinly sputter-coated with carbon using Polaron E5100 sputter coater. The pore sizes of the hydrogels were measured from the FE-SEM images using image analysis software (ImageJ).

2.10 Statistical analysis

Results are presented as means ± standard deviation. Each loading of either MCNF or CMCNF was compared to the alginate using two-sample t-test on OriginPro 2018 software. The difference between means is considered significant when $p < 0.05$.

3. Results and Discussion

3.1 Gelation and Homogeneity

In this study, $CaCl_2$ enriched agar gels were used to control the gelation of SA by allowing slower diffusion of the calcium ions from the agar gels into the SA solutions. Visual observations of the hydrogels showed that the crosslinking process initially began from the outer circumference of the alginate solution in contact with the agar mould, before gradually diffusing into the inner circumference of the solution. The effect of gelation temperature and the duration of crosslinking on the homogeneity of the neat SA hydrogels can be seen from

Fig. 1A (crosslinked for 24 h at 4 °C, 25 °C and 37°C) and Fig. 1B (crosslinked at 4°C for 24 h, 48 h and 72 h).

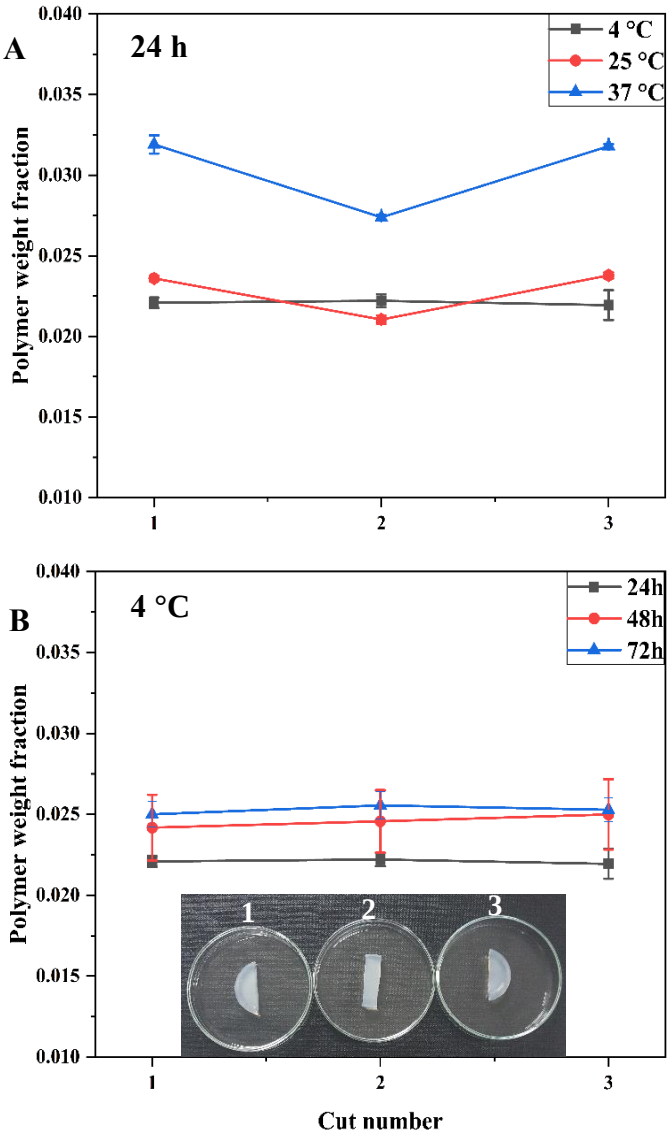

Fig. 1: Effect of temperature (A) and time (B) on the homogeneity of SA hydrogels. Photographic insert of the equilibrium swollen hydrogel cuts

There was no significant change in the polymer weight fractions across the three cuts of the hydrogels prepared at 4 °C as shown in Fig. 1A, indicating a homogeneous network formation within the gels. This can be attributed to the slower diffusion of the calcium ions from the agar gels into the SA solution at 4 °C. These hydrogels also had reduced shrinkage at the end of the crosslinking process. However, when the SA solution was crosslinked at 25 °C and 37 °C, heterogeneous hydrogels resulted, with the mid-point of the hydrogels (cut number 2) having a lower polymer fraction compared to the outer cuts. The reduction in polymer fraction at the

midpoint of the hydrogels was very significant for the hydrogels prepared at 37 °C, directly implying a higher water content and reduced crosslinking density at the mid-point of the hydrogel. These results and observations show that the temperature of gelation plays a major role on the homogeneity of these hydrogels when using the agar gel moulds.

The various durations of gelation at 4 °C do not have any significant effect on the polymer weight fractions across the three cuts as shown in Fig. 1B, implying that the duration of crosslinking does not affect the homogeneity of the hydrogels. Henceforth, the composite hydrogels reported herein are for those crosslinked at 4 °C for a 24 h period.

3.2 Surface interaction from FTIR analysis

FTIR analysis was carried out to probe the interaction between the sodium alginate and the two types of CNF upon crosslinking. The overlay of the FTIR spectrum for SA_MCNF and SA_CMCNF composite hydrogels are shown in Fig. 2A and 2B respectively. All the spectrum from the composite hydrogels presented the same peaks as the alginate matrix. The broad peaks identified in all the spectrum between 3227-3335 cm^{-1} were assigned to the O-H stretching vibrations, while the peaks identified between 2924 - 2902 cm^{-1}, 1590 - 1587 cm^{-1}, 1414 - 1411 cm^{-1} and 1024 -1015 cm^{-1} were assigned to the C-H, COO^- (asymmetric), COO^- (symmetric) and C-O stretching vibrations respectively (Sirviö, Kolehmainen, Liimatainen, Niinimäki, & Hormi, 2014).

A shift in the O-H stretching vibration to higher wavenumber was seen for SA_MCNF_10 and SA_MCNF_20 (from 3227 to 3264 cm^{-1}) and for SA_CMCNF_10 and SA_CMCNF_20 (from 3227 to 3266 cm^{-1}), indicating an increase in the O-H functional groups, as the percentage loadings of both CNFs increases. There were significant shifts of the C-O peak from 1024 cm^{-1} to 1020 cm^{-1}, and 1024 cm^{-1} to 1017 cm^{-1} for SA_MCNF_10 and SA_MCNF_20 respectively. A similar shift to lower wavenumber of the C-O peak was seen with alginate film having 50 % microfibrillated cellulose and was attributed to an interaction between alginate and residual hemicellulose (Sirviö et al., 2014). However, the conclusion of the authors cannot be adopted in this case as the cellulose material used for the preparation of the MCNF was from dissolving pulp, having negligible hemicellulose content. These shifts toward lower wavenumbers at these percentage loadings imply an interaction between alginate and MCNF at lower bond energy in comparison with the pure alginate.

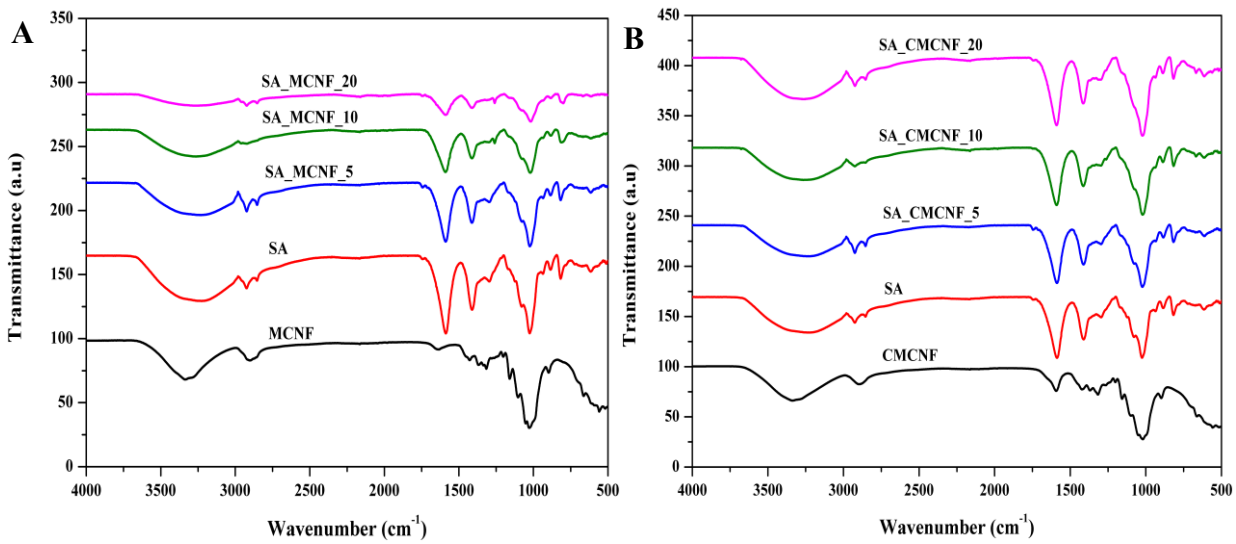

Fig. 2: FTIR spectrum overlay of SA_MCNF and SA_CMCNF composite hydrogels with each of the starting materials

It was of interest to investigate whether the carboxymethyl groups of CMCNF at the amounts studied interacted with the alginate in such a way as to contribute to ionic crosslinking as has been reported for carboxyl groups of TEMPO oxidised CNF (Lin et al., 2012). This would be observed as a shift in the asymmetric and symmetric peaks of COO^- groups. There was only a 3 cm^{-1} shift to higher wavenumber for SA_CMCNF_20, which is considered statistically significant. Therefore, it can be assumed that there is an interaction between alginate and CMCNF at the COO^- functional group for SA_CMCNF_20, which may have some minor contribution to ionic crosslinking. There was no significant shift in the peaks of all other observable functional groups of alginates with the addition of CMCNF at different percentage loadings.

3.3 Effect of CNF loadings on the swelling of never-dried hydrogels in water

The amount of water imbibed by a three-dimensional network alginate hydrogel system would depend on the amount of free hydrophilic hydroxyl groups which are not participating in ionic crosslinking and on the degree of crosslinking, in other words, the void spaces created within the hydrogels after crosslinking (Draget, Skjåk-Bræk, & Smidsrød, 1997). The effects of varying loadings of the CNF materials on the swelling degree of SA hydrogels from never-dried samples were studied by swelling the hydrogels to an equilibrium state in water and the results presented in Table 1.

Table 1: Swelling degree, storage modulus and crosslinking degree parameters of the alginate-based composite hydrogels.

Sample	**Swelling degree**	**Storage modulus, *G'* (kPa) @ 1 Hz**	ν_e **(mol/cm^3)**
SA	42.6 ±0.8	44.5 ±0.0	6.9E-4 ±2.0E-5
SA_MCNF_5	38.0 ±1.9	56.4 ±4.5	8.5E-4 ±1.9E-5
SA_MCNF_10	40.3 ±1.5	54.6 ±4.8	7.8E-4 ±1.4E-5
SA_MCNF_20	39.2 ±0.4	56.4 ±9.5	5.5E-4 ±1.6E-5
SA_CMCNF_5	44.8 ±0.5	48.9 ±3.4	7.9E-4 ±3.7E-5
SA_CMCNF_10	45.8 ±0.1	50.4 ±0.5	6.8E-4 ±4.6E-5
SA_CMCNF_20	42.5 ±2.2	64.7 ±9.9	6.9E-4 ±7.6E-5

The addition of MCNF at all the percentage loadings studied led to an overall significant reduction in the swelling degree of SA_MCNF hydrogels in comparison to the neat SA hydrogel. The least swelling degree was observed for SA_MCNF_5 and 11 % lower than neat SA hydrogel. The reduction in swelling was also reported by Huq et al. (2012) with the addition of 5 wt. % cellulose nanocrystals to sodium alginate films and was attributed to an increase in mechanical property.

On the other hand, the swelling degree of SA_CMCNF_5 and SA_CMCNF_10 were significantly improved when compared to the neat SA, whereas no change in swelling degree was observed for SA_CMCNF_20. Similar increase in aqueous swelling behaviour was observed by Lin et al., (2014) when increasing the amount of carboxymethylated bacterial cellulose in alginate-based hydrogels. The increase in swelling was attributed to the presence of the anionic hydrophilic carboxymethyl groups on the surface of CMCNF. The anionic groups which are not contributing to ionic crosslinking bring about electrostatic repulsive forces on the fibre surface, which promotes fibre swelling, and adds to the overall swelling degree of the hydrogels. These anionic groups are however not present on the surface MCNF and do not contribute to the swelling, hence the observed reduced swelling.

3.4 Effect of the CNF materials on the viscoelastic properties of the alginate-based hydrogels

The *G'* of the hydrogels at 1 Hz are presented in Table 1. In addition, the overlay of the frequency sweeps of the SA_MCNF and SA_CMCNF composite hydrogels at a constant strain value of 0.01% are shown in Fig. 3. All the composite hydrogels studied show a higher storage modulus (*G'*) than loss modulus (*G''*), an indication of complete gelled network material (Magami, 2017). In addition, the *G'* of all the hydrogels are almost independent of the frequency applied which is also a prevalent characteristic of a gelled network system.

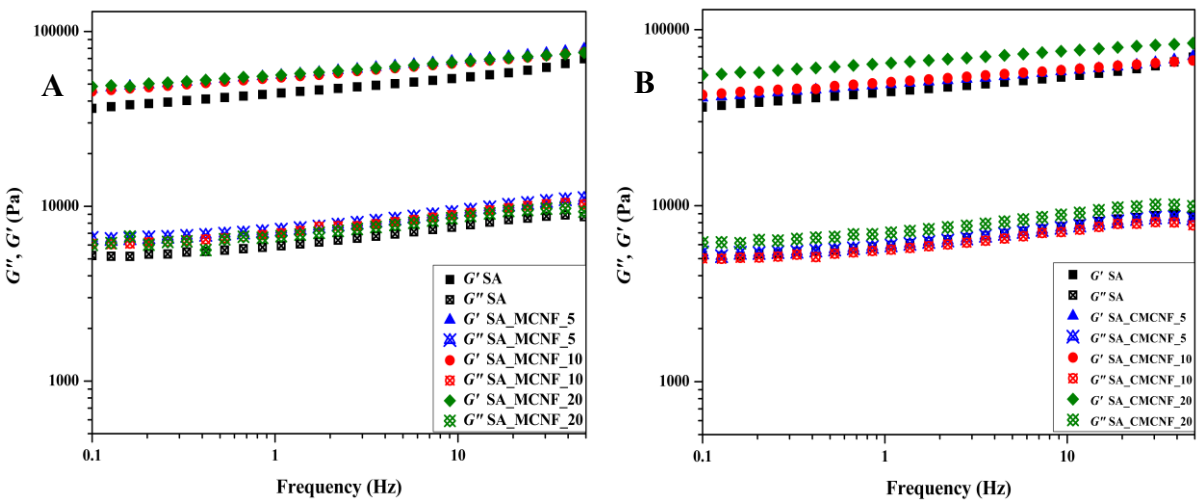

Fig. 3: Overlay of frequency sweeps of SA_MCNF (A) and SA_CMCNF (B) hydrogels

The addition of 5 wt. % MCNF led to a 27 % increase in *G'* compared to the neat SA hydrogel, further increases in the percentage loading of MCNF did not result in a significant effect on the storage modulus of the hydrogels. On the other hand, the addition of 5 wt. % CMCNF led to a 10 % increase in *G'* compared to the neat SA hydrogel. The higher storage modulus of SA_MCNF_5 in comparison to the SA_CMCNF_5 suggests a higher reinforcing ability of MCNF compared to CMCNF. The higher storage modulus could also explain the low swelling degree of SA_MCNF composite hydrogels. Although the increase in *G'* was lower for SA_CMCNF_5, there was a linear and significant increase in the storage modulus with further increases in the amounts CMCNF. The significant increase in *G'* with the addition of 10 wt. % and 20 wt. % CMCNF can be attributed to the presence of the anionic carboxymethyl groups which have the potentials to contribute to the gel-like behaviour of alginate, given that carboxymethylated cellulose (CMC) is a well-known rheology modifier.

3.5 Effect of CNF materials on the compressive modulus and elastically effective chains of alginate-based hydrogels

The mechanical properties of the hydrogels were further characterised by carrying out compression tests on the equilibrium-swollen hydrogels. An overlay of the plot of stress vs deformation factor for all the hydrogel is shown in Fig. 4.

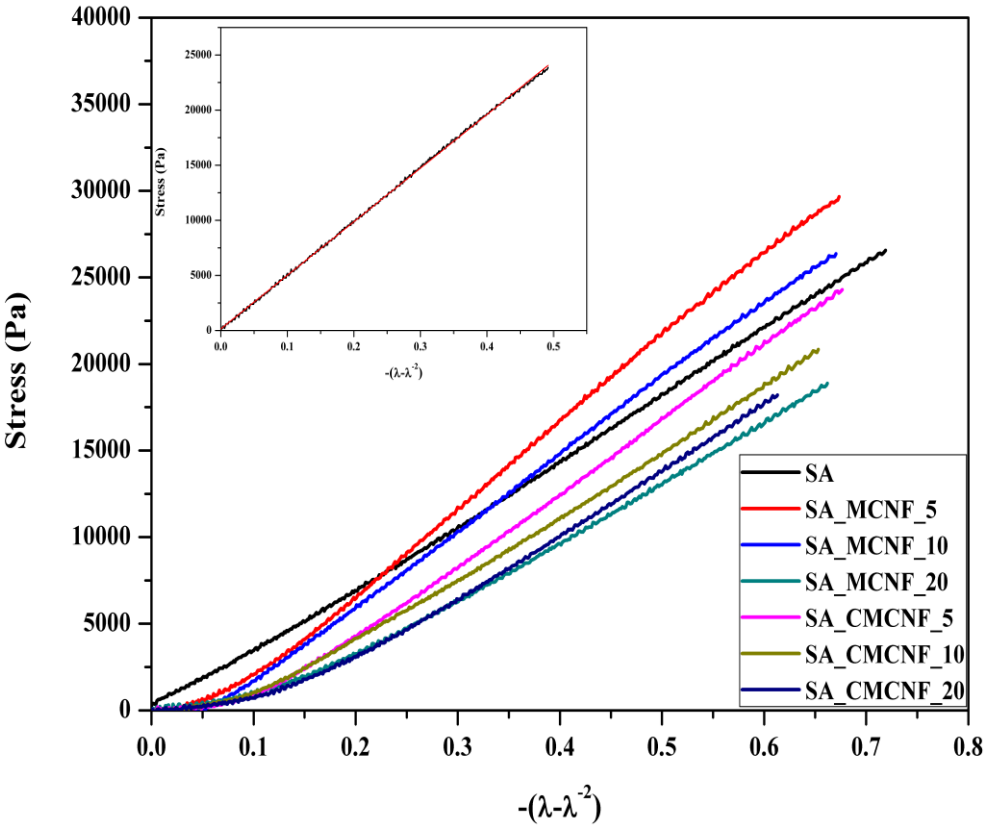

Fig. 4: Stress-deformation factor relationship of all hydrogels with a representative insert of the corrected plot without a toe region.

All hydrogels tested showed a toe region at the beginning of the test, up to 10 % deformation, before showing a linear relationship between stress and deformation factor. The toe region manifests because of imperfect hydrogel surface as the upper platen of the rheometer makes contact with the entire area of the hydrogel cylinder (Muniz & Geuskens, 2001). It was observed that 0.1 N normal force was enough to make good contact with the hydrogels. Subsequently, the data set was corrected by subtracting the value of stress and deformation factor at 0.1 N from all data set, to obtain the plot shown as the insert image (representative image) on Fig. 4. The linear fit of the plot was then carried out using OriginPro 2018 software and the slope of the plot reported as the compressive modulus (*G*).

The compressive modulus of SA, SA_MCNF and SA_CMCNF hydrogels are shown in Fig. 5. The hydrogel composite materials showed highest compressive modulus at 5 wt. % MCNF and CMCNF loadings. The addition of 5 wt. % MCNF resulted in a 36 % increase in compressive modulus of the hydrogels in comparison with the neat SA hydrogel, while a 17 % increase in compressive modulus was observed with the addition of CMCNF at the same percentage loading. This result confirms that MCNF is more efficient in reinforcing SA than CMCNF.

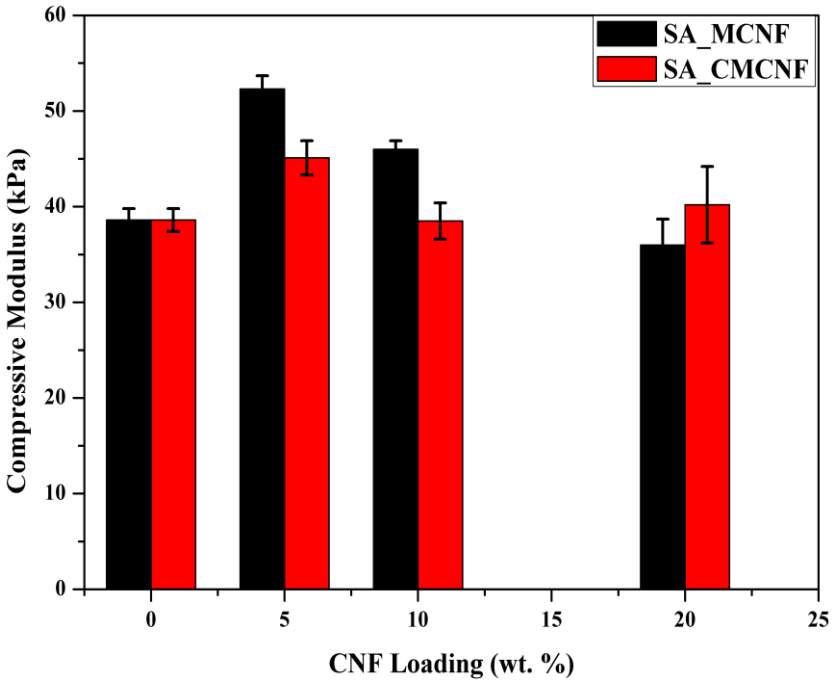

Fig. 5: Compressive modulus of SA_MCNF and SA_CMCNF hydrogels

The SA_MCNF_10 and SA_MCNF_20 hydrogels with lower swelling degree and higher storage modulus are also expected to have higher compressive modulus in comparison to the neat SA hydrogels. However, lower compressive moduli were seen for these samples. It should be noted that at 10 wt. % (0.002 wt. fraction) and 20 wt. % (0.004 wt. fraction) MCNF and CMCNF loadings, the fibrils are beyond the respective connectivity threshold of 0.0014 wt. fraction and 0.00065 wt. fraction (Onyianta et al., 2018). Therefore, there is a tendency for the fibrils to form aggregates within the hydrogels, leading to network imperfection. The compressive deformation imposed on the hydrogels appears to be more sensitive to these fibrillar aggregation occurring at higher percentage loading of the CNF materials. These fibrillar aggregations and entanglements seems to have offset any reinforcing capacity accrued at lower percentage loading. The rotational shearing force imposed during the frequency sweeps might not have identified the presence of fibril kinks and aggregation but able to detect

the increase in the solid-like component of the hydrogels. Hence, the *G'* is seen to plateau or increase linearly when the respective amount of MCNF and CMCNF is increased.

To further elucidate the effect of the CNF materials on SA hydrogels' network structure, the modified Flory's equation for rubber elasticity was used to calculate the moles per cm^3 of the elastically effective chains within the SA_CNF composite hydrogels. This equation basically relates the compressive modulus with the inverse of equilibrium swelling degree as shown in Equation 5. The effect of the CNF type and loading on the moles of elastically effective chains of the hydrogels is shown in Table 1. An increase in the elastically effective chains of SA_MCNF_5 and SA_MCNF_10 when compared to the neat alginate was observed. This increase is an indication of the formation of physical networks, through intermolecular interactions. However, at 20 wt. % MCNF, aggregation of fibrils begins to occur, resulting in the formation of imperfects, hence the low ν_e.

Also, there was an increase in ν_e for SA_CMCNF_5, however, there was no significant change in the elastically effective chains of SA_CMCNF_10 and SA_CMCNF_20. Although the FTIR data analysis suggested a possible minor contribution in ionic crosslinking for SA_CMCNF_20, these crosslinks if presents, may not have been elastically effective. Thereby explaining the insignificant change in the compressive modulus of the sample.

3.6 Morphological properties of SA_CNF composite hydrogels.

The hydrogel with the highest compressive modulus for each CNF type was probed to identify the degree and nature of pores created upon equilibrium swelling in water and freeze-drying. The cross-sectional images of SA, SA_MCNF_5 and SA_CMCNF_5 samples are shown in Fig. 6, having a respective average porous size of 114 ±46 µm, 84 ±43 µm and 157 ±86 µm.

The incorporation of MCNF into the SA hydrogel resulted in a rather compact and distinct layered structure, having lower average pore size than the neat SA hydrogel and the SA_CMCNF_5 hydrogel, which both have network structures that are more porous. The surface repulsive carboxymethyl groups alongside the carboxyl groups on SA would result in a net increased void spaces within the polymer, leading to larger intake of water. Whereas the attractive hydroxyl groups on the surface of the MCNF would lead to an increased inter and intramolecular attraction of the fibrils within the SA_MCNF_5 composite, hence the observed lower porosity relative to the neat SA hydrogel. This explains the reduced water uptake of SA_MCNF_5 hydrogel when compared to SA and SA_CMCNF_5 hydrogels as shown in Table 1.

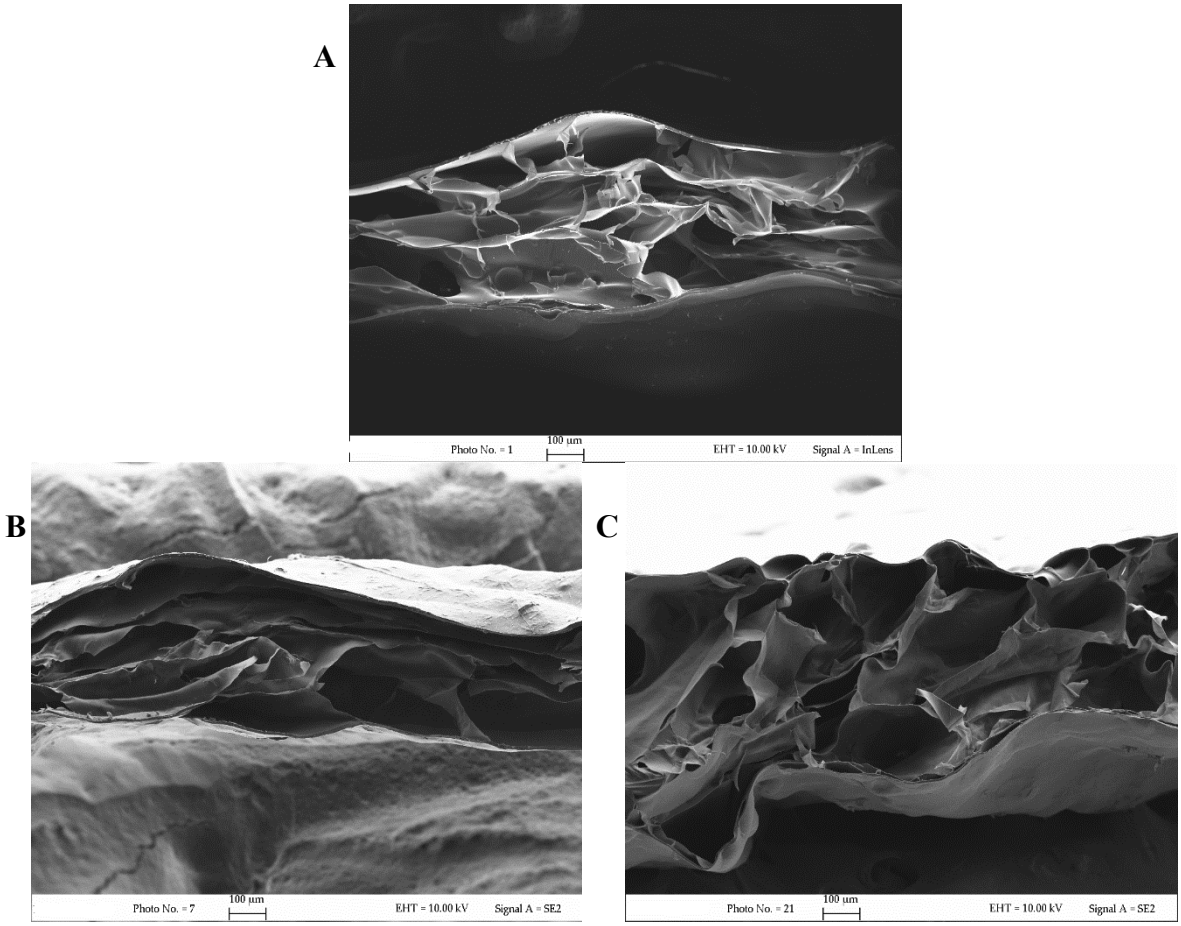

Fig. 6: Cross-sectional FE-SEM images of SA hydrogel (A), SA_MCNF_5 (B) and SA_CMCNF_5 (C)

Conclusions

The use of calcium chloride enriched agar gel moulds at 4 °C resulted in the formation of homogeneously crosslinked alginate. The addition of 5 wt. % MCNF led to a 36 % increase in compressive modulus, an increase in the elastically effective chains and storage modulus. In addition, the SA_MCNF_5 composite hydrogel had less porous structure, because of the lack of anionic repulsive groups on the surface of MCNF, which contributed to the observed reduced swelling in water. On the other hand, the presence of anionic carboxymethyl groups on the surface of the CMCNF led to a slightly improved swelling degree, a more porous network structure, having smaller increases in the compressive modulus, elastically effective chains and storage modulus when compared to the neat alginate hydrogel. These positive effects were observed at lower percentage loadings of the CNFs (5 wt. %). Increasing the percentage loadings however did not lead to improvement in material properties of the hydrogels, due to possible fibril aggregation. Therefore, only 5 wt. % CNF materials are required to prepare

alginate hydrogels that could find applications in areas where good swelling and mechanical strength are needed.

Acknowledgement

The authors would like to thank the Edinburgh Napier University for the anniversary studentship. They are also grateful to Laura Negretti and Giulia Gaggero for helping with the FE-SEM images.

References

Abdul Khalil, H. P. S., Davoudpour, Y., Islam, M. N., Mustapha, A., Sudesh, K., Dungani, R., & Jawaid, M. (2014). Production and modification of nanofibrillated cellulose using various mechanical processes: A review. *Carbohydrate Polymers*, *99*, 649–665. https://doi.org/10.1016/j.carbpol.2013.08.069

Ahmed, E. M. (2015). Hydrogel: Preparation, characterization, and applications: A review. *Journal of Advanced Research*, *6*(2), 105–121. https://doi.org/10.1016/j.jare.2013.07.006

Akagi, Y., Katashima, T., Katsumoto, Y., Fujii, K., Matsunaga, T., Chung, U. Il, … Sakai, T. (2011). Examination of the theories of rubber elasticity using an ideal polymer network. *Macromolecules*. https://doi.org/10.1021/ma201088r

Aravamudhan, A., Ramos, D. M., Nada, A. A., & Kumbar, S. G. (2014). Chapter 4 - Natural Polymers: Polysaccharides and Their Derivatives for Biomedical Applications. In M. Kumbar, Sangamesh G.; Laurencin, Cato T.; Deng (Ed.), *Natural and Synthetic Biomedical Polymers* (pp. 67–89). Elsevier. https://doi.org/https://doi.org/10.1016/B978-0-12-396983-5.00004-1

Augst, A. D., Kong, H. J., & Mooney, D. J. (2006). Alginate hydrogels as biomaterials. *Macromolecular Bioscience*, *6*(8), 623–633. https://doi.org/10.1002/mabi.200600069

Aulin, C., Johansson, E., Wågberg, L., & Lindström, T. (2010). Self-organized films from cellulose i nanofibrils using the layer-by-layer technique. *Biomacromolecules*, *11*(4), 872–882. https://doi.org/10.1021/bm100075e

Bajpai, M., Shukla, P., & Bajpai, S. K. (2016). Ca(II)+Ba(II) ions crosslinked alginate gels prepared by a novel diffusion through dialysis tube (DTDT) approach and preliminary BSA release study. *Polymer Degradation and Stability*. https://doi.org/10.1016/j.polymdegradstab.2016.09.027

Beyene, D., Chae, M., Dai, J., Danumah, C., Tosto, F., Demesa, A. G., & Bressler, D. C. (2017). Enzymatically-Mediated Co-Production of Cellulose Nanocrystals and Fermentable Sugars. *Catalysts* . https://doi.org/10.3390/catal7110322

Cardoso, M. J., Costa, R. R., & Mano, J. F. (2016). Marine origin polysaccharides in drug delivery systems. *Marine Drugs*, *14*(2), 1–27. https://doi.org/10.3390/md14020034

Draget, K. I., Skjåk-Bræk, G., & Smidsrød, O. (1997). Alginate based new materials. *International Journal of Biological Macromolecules*, *21*(1–2), 47–55. https://doi.org/10.1016/S0141-8130(97)00040-8

Flory, P. J. (1953). Chapter XI: Rubber Elasticity. In P. J. Flory (Ed.), *Principles of Polymer Chemistry* (pp. 432–493).

Goodwin, J. W., & Hughes, R. W. (2008). *Rheology for Chemists*. Royal Society of Chemistry. https://doi.org/10.1039/9781847558046

Guilherme, M. R., Aouada, F. A., Fajardo, A. R., Martins, A. F., Paulino, A. T., Davi, M. F. T., … Muniz, E. C. (2015). Superabsorbent hydrogels based on polysaccharides for application in agriculture as soil conditioner and nutrient carrier: A review. *European Polymer Journal*, *72*, 365–385. https://doi.org/10.1016/j.eurpolymj.2015.04.017

Hubbe, M. A., Ferrer, A., Tyagi, P., Yin, Y., & Salas, C. (2017). com Nanocellulose in Thin Films, Coatings, and Plies for Packaging Applications: A Review, *12*, 2143–2233.

Huq, T., Fraschini, C., Khan, A., Riedl, B., Bouchard, J., & Lacroix, M. (2017). Alginate based nanocomposite for microencapsulation of probiotic: Effect of cellulose nanocrystal (CNC) and lecithin. *Carbohydrate Polymers*, *168*, 61–69. https://doi.org/10.1016/j.carbpol.2017.03.032

Huq, T., Salmieri, S., Khan, A., Khan, R. A., Le Tien, C., Riedl, B., … Lacroix, M. (2012). Nanocrystalline cellulose (NCC) reinforced alginate based biodegradable nanocomposite film. *Carbohydrate Polymers*, *90*(4), 1757–1763. https://doi.org/10.1016/j.carbpol.2012.07.065

Isogai, A., Saito, T., & Fukuzumi, H. (2011). TEMPO-oxidized cellulose nanofibers. *Nanoscale*, *3*(1), 71–85. https://doi.org/10.1039/C0NR00583E

Jonoobi, M., Oladi, R., Davoudpour, Y., Oksman, K., Dufresne, A., Hamzeh, Y., & Davoodi, R. (2015). Different preparation methods and properties of nanostructured cellulose from various natural resources and residues: a review. *Cellulose*, *22*(2), 935–969. https://doi.org/10.1007/s10570-015-0551-0

Klemm, D., Kramer, F., Moritz, S., Lindström, T., Ankerfors, M., Gray, D., & Dorris, A. (2011). Nanocelluloses: A new family of nature-based materials. *Angewandte Chemie - International Edition*, *50*(24), 5438–5466. https://doi.org/10.1002/anie.201001273

Kong, H. J., & Mooney, D. J. (2003). The Effects of Poly(Ethyleneimine) (PEI) Molecular Weight on Reinforcement of Alginate Hydrogels. *Cell Transplantation*. https://doi.org/10.3727/000000003108747253

Kuo, C. K., & Ma, P. X. (2001). Ionically crosslinked alginate hydrogels as scaffolds for tissue engineering: Part 1. Structure, gelation rate and mechanical properties. *Biomaterials*, *22*(6), 511–521. https://doi.org/10.1016/S0142-9612(00)00201-5

Lee, S. B., Seo, S. M., Lim, Y. M., Cho, S. K., Lee, Y. M., & Nho, Y. C. (2004). Preparation of alginate/poly(N-isopropylacrylamide) hydrogels using gamma-ray irradiation grafting. *Macromolecular Research*, *12*(3), 269–275. https://doi.org/10.1007/BF03218399

Leppiniemi, J., Lahtinen, P., Paajanen, A., Mahlberg, R., Metsä-Kortelainen, S., Pinomaa, T., … Hytönen, V. P. (2017). 3D-Printable Bioactivated Nanocellulose-Alginate Hydrogels. *ACS Applied Materials and Interfaces*, *9*(26), 21959–21970. https://doi.org/10.1021/acsami.7b02756

Lin, N., Bruzzese, C., & Dufresne, A. (2012). TEMPO-oxidized nanocellulose participating as crosslinking aid for alginate-based sponges. *ACS Applied Materials and Interfaces*, *4*(9), 4948–4959. https://doi.org/10.1021/am301325r

Lin, Q., Zheng, Y., Ren, L., Wu, J., Wang, H., An, J., & Fan, W. (2014). Preparation and characteristic of a sodium alginate/carboxymethylated bacterial cellulose composite with a crosslinking semi-interpenetrating network. *Journal of Applied Polymer Science*, *131*(3), 1–9. https://doi.org/10.1002/app.39848

Ma, X., Li, R., Zhao, X., Ji, Q., Xing, Y., Sunarso, J., & Xia, Y. (2017). Biopolymer composite fibres composed of calcium alginate reinforced with nanocrystalline cellulose. *Composites Part A: Applied Science and Manufacturing*, *96*, 155–163. https://doi.org/10.1016/j.compositesa.2017.02.021

Magami, S. M. (2017). In situ viscoelasticity and in situ thermo- responsiveness in acrylic acid-based soft hydrogels In situ viscoelasticity and in situ thermo-responsiveness in acrylic acid-based soft hydrogels. In *IOP Conference Series: material Science and Engineering*. https://doi.org/10.1088/1757-899X/264/1/012019

Muniz, E. C., & Geuskens, G. (2001). Compressive elastic modulus of polyacrylamide hydrogels and semi-IPNs with poly(N-isopropylacrylamide). *Macromolecules*, *34*(13), 4480–4484. https://doi.org/10.1021/ma001192l

Onyianta, A. J., Dorris, M., & Williams, R. L. (2018). Aqueous morpholine pre-treatment in cellulose nanofibril (CNF) production: comparison with carboxymethylation and TEMPO oxidisation pre-treatment methods. *Cellulose*, *25*(2), 1047–1064. https://doi.org/10.1007/s10570-017-1631-0

Park, S. Bin, Lih, E., Park, K. S., Joung, Y. K., & Han, D. K. (2017). Biopolymer-based functional composites for medical applications. *Progress in Polymer Science*, *68*, 77–105. https://doi.org/10.1016/j.progpolymsci.2016.12.003

Sannino, A., Pappadà, S., Madaghiele, M., Maffezzoli, A., Ambrosio, L., & Nicolais, L. (2005). Crosslinking of cellulose derivatives and hyaluronic acid with water-soluble carbodiimide. *Polymer*. https://doi.org/10.1016/j.polymer.2005.10.048

Sirviö, J. A., Kolehmainen, A., Liimatainen, H., Niinimäki, J., & Hormi, O. E. O. (2014). Biocomposite cellulose-alginate films: Promising packaging materials. *Food Chemistry*, *151*, 343–351. https://doi.org/10.1016/j.foodchem.2013.11.037

Smyth, M., M'Bengue, M. S., Terrien, M., Picart, C., Bras, J., & Foster, E. J. (2018). The effect of hydration on the material and mechanical properties of cellulose nanocrystal-alginate composites. *Carbohydrate Polymers*, *179*(September 2017), 186–195. https://doi.org/10.1016/j.carbpol.2017.09.002

Stagnaro, P., Schizzi, I., Utzeri, R., Marsano, E., & Castellano, M. (2018). Alginate-polymethacrylate hybrid hydrogels for potential osteochondral tissue regeneration. *Carbohydrate Polymers*. https://doi.org/10.1016/j.carbpol.2018.01.012

Vicini, S., Castellano, M., Mauri, M., & Marsano, E. (2015). Gelling process for sodium alginate: New technical approach by using calcium rich micro-spheres. *Carbohydrate Polymers*, *134*, 767–774. https://doi.org/10.1016/j.carbpol.2015.08.064

Vicini, S., Mauri, M., Wichert, J., & Castellano, M. (2017). Alginate gelling process: Use of bivalent ions rich microspheres. *Polymer Engineering and Science*. https://doi.org/10.1002/pen.24552

Wågberg, L., Decher, G., Norgren, M., Lindström, T., Ankerfors, M., & Axnäs, K. (2008). The buildrs of microfibrillated cellulose and cationic polyelectr-up of polyelectrolyte multilayeolytes. *Langmuir*, *24*(3), 784–795. https://doi.org/10.1021/la702481v